Tanaya Datta,
Palukuru Nagendra*,
Sunita Halder nee Dey,
Subrata Paul

J. Electrical Systems 9-4 (2013): 440-452

Regular paper

Voltage stability assessment of a power system incorporating FACTS in equivalent mode

JES
Journal of Electrical Systems

Two-bus network equivalent is commonly used to get a quick overview on the voltage stability of a multi-bus power system. This paper presents a method to predict the voltage collapse point of power system incorporating two major FACTS devices i.e., Static VAR Compensator (SVC) and Static Synchronous Compensator (STATCOM) using a two-bus integrated equivalent system. The proposed methodology has been applied under simulated condition on IEEE 57-bus test system to illustrate its effectiveness using a voltage stability indicator being derived from developed equivalent model. Voltage stability margin augmentation with the application of SVC and STATCOM is compared with the system having no compensation.

Keywords: Equivalent two-bus system; voltage stability index; SVC; STATCOM; weakest bus.

1. Introduction

Due to economic and environmental pressures, present day power systems have become highly complex and are operated closer to their operating limits and therefore vulnerable to stability and security problems. Voltage stability is the main issue with such stressed systems and is referred as the ability of power system to maintain acceptable voltage level at all the buses in the system under normal conditions or after being subjected to a disturbance. Reports of the occurrence of voltage collapse are becoming more frequent in such stressed systems and this problem has been an area of great interest to power system researchers [1]. A system is said to enter a state of voltage instability when a disturbance, increase in load or a change in system conditions causes a progressive and uncontrollable drop in voltage. The uncontrolled voltage decline at system load buses may cause a series of line outages and the ultimate result is system blackout. It is well recognized that voltage collapse normally occurs when there exists a large demand of power especially reactive power [2,3], but at exactly what load level the failure will occur is not easily predicted.

Several approaches have been reported in the open literature for the prediction of voltage instability and collapse of the power system [4-7]. Voltage stability analysis often requires examination of lots of system states and many contingency scenarios. For this reason, the approach based on steady state analysis is more feasible, and it can also provide insights of the voltage or reactive power problems.

Gradually the concept of deriving two bus equivalent system [8] of any multi-bus power network has come and several voltage stability indicators have been developed using Thevenin's equivalent circuit [8-11] to get quick overview on the system voltage instability. Some of the two bus equivalent methodologies [12-16] developed are also capable to predict better scheme for strategic load shedding based on voltage stability criterion instead on the ground of the simple voltage magnitude criterion.

* Corresponding author: Dr. Palukuru Nagendra, E-mail: nagendra_ju@rediffmail.com is with the Department of Technical Education, A. P. , Hyderabad.
Authors are with the Department of Electrical Engineering, Jadavpur University, Kolkata 700032, INDIA.

Flexible AC Transmission System (FACTS) was launched to solve the emerging system problems [16,17]. FACTS controllers are used to regulate power flow, transmission voltage and through rapid control action can mitigate dynamic disturbances. Static Var Compensators (SVC) and Static Synchronous Compensator (STATCOM) are widely used for shunt reactive compensation in order to maintain a flat voltage profile. Others such as Thyristor Controlled Series Capacitor (TCSC) and Static Synchronous Series Compensator (SSSC) are used to control the power flow through transmission lines. To analyse the effect of these controllers in power system analysis, steady state models have been developed over the decade [17-20]. Power flow analysis of systems using such models would provide data necessary to calculate voltage collapse indicators in order to evaluate the response of the system.

With the concept of network equivalence [12-16] available in literature, an attempt is made in this paper to describe a method of equivalencing a multi-bus power network to a series equivalent two-bus system developed from the Newton-Raphson power flow with integrated mathematical model of two FACTS controllers (SVC and STATCOM) and thereby voltage stable states of the entire system following the load changes in 'weak' load buses investigated for two typical power system networks. Voltage stability enrichment using these two FACTS controllers have been compared based on the test systems under simulation. The simulation also includes the detection of the 'weak' load bus/buses and identification of the global voltage stable states of the system following the derived two-bus equivalent system simulation. An IEEE 57-bus system has been used to illustrate the application of proposed concept.

2. Modelling of FACTS Controllers

2.1 Static Var Compensator

SVC firing angle model has been used here for power flow analysis [17,18]. It is made up of the parallel combination of a thyristor controlled reactor (TCR) and a fixed capacitor. SVC connected to the transmission network via a step-down transformer is shown in Fig.1.

The SVC is considered as a continuous, shunt variable susceptance, which is adjusted in order to achieve a specified voltage magnitude while satisfying constraint conditions. Suitable control of this equivalent reactance is brought about by varying the current through the TCR by controlling the gate firing instant of the thyristors and thus the equivalent susceptance B_{t_svc} is thus a function of the firing angle α. The SVC effective reactance X_{svc} is determined by the parallel combination of X_C and X_{tcr} and is given by

$$X_{svc} = \frac{X_C X_L}{\frac{X_C}{\pi}\left(2\left(\pi-\alpha\right)+\sin\left(2\alpha\right)\right)-X_L}$$

The partial derivatives required to calculate load flow Jacobian with respect to the SVC (connected at m^{th} bus) firing angle α are,

$$\frac{\partial P_m}{\partial \alpha} = \frac{\partial P_{t\_svc}}{\partial \alpha} = V_m^2 \frac{\partial G_{t\_svc}}{\partial \alpha}$$

$$\frac{\partial Q_m}{\partial \alpha} = \frac{\partial Q_{t\_svc}}{\partial \alpha} = -V_m^2 \frac{\partial B_{t\_svc}}{\partial \alpha}$$

P_m= *active power injected by lines connected to the node* + P_{t_svc},

Q_m= *reactive power injected by lines connected to the node* + Q_{t_svc}.

where P_m and Q_m are net active and reactive powers injected at bus *m*

Here,

$$\frac{\partial G_{t\_svc}}{\partial \alpha} = -\frac{R_t}{DT^2}\frac{\partial DT}{\partial \alpha}; \quad \frac{\partial B_{t\_svc}}{\partial \alpha} = \frac{-DT\dfrac{\partial X_{svc}}{\partial \alpha} + X_{eq}\dfrac{\partial DT}{\partial \alpha}}{DT^2};$$

$$\frac{\partial X_{svc}}{\partial \alpha} = \frac{2X_{svc}^2}{\pi X_L}\left(1-\cos(2\alpha)\right); \quad \frac{\partial DT}{\partial \alpha} = 2X_{eq}\frac{\partial X_{svc}}{\partial \alpha}; \text{ and } DT = R_t^2 + X_{eq}^2$$

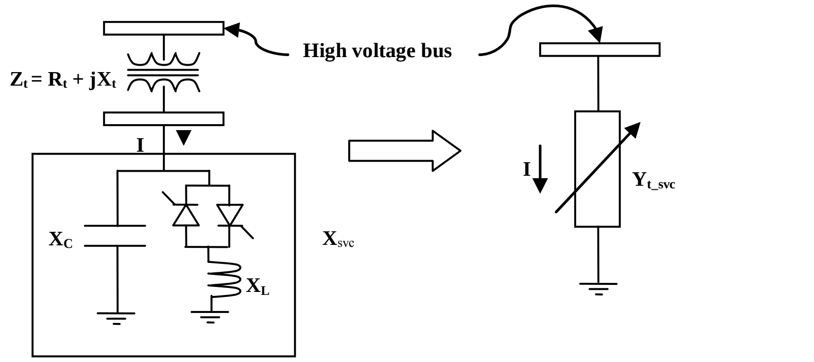

Fig.1. SVC connected to transmission network via a step-down transformer

The implementation of the variable shunt susceptance models in a Newton-Raphson load flow program has required the incorporation of a non-standard type of bus, namely PV bus. This is a controlled bus where the nodal voltage magnitude and active and reactive powers are specified whilst the SVC's firing angle α is handled as state variable. If *α* is within limits ($90^0 \le \alpha \le 180^0$), the specified voltage magnitude is attained and the controlled bus remains a PV type bus. However, if *α* goes out of limits, it is fixed at the violated limit and the bus becomes a PQ type bus with fixed susceptance connected to it. The linearized power flow equations for a system of N buses with svc at m^{th} bus are given below:

$$\begin{bmatrix} \Delta P_2 \\ \vdots \\ \Delta P_m \\ \vdots \\ \Delta P_N \\ \Delta Q_2 \\ \vdots \\ \Delta Q_N \\ \Delta Q_m \end{bmatrix} = \begin{bmatrix} \frac{\partial P_2}{\partial \delta_2} & \cdots & \frac{\partial P_2}{\partial \delta_m} & \cdots & \frac{\partial P_2}{\partial \delta_N} & |V_2|\frac{\partial P_2}{\partial |V_2|} & \cdots & |V_N|\frac{\partial P_2}{\partial |V_N|} & 0 \\ \vdots & \vdots & \vdots & \vdots & \vdots & \vdots & \vdots & \vdots & \vdots \\ \frac{\partial P_m}{\partial \delta_2} & & \frac{\partial P_m}{\partial \delta_m} & \cdots & \frac{\partial P_m}{\partial \delta_N} & |V_2|\frac{\partial P_m}{\partial |V_2|} & \cdots & |V_N|\frac{\partial P_m}{\partial |V_N|} & \frac{\partial P_m}{\partial \alpha} \\ \vdots & \vdots & \vdots & \vdots & \vdots & \vdots & \vdots & \vdots & \vdots \\ \frac{\partial P_N}{\partial \delta_2} & \cdots & \frac{\partial P_N}{\partial \delta_m} & \cdots & \frac{\partial P_N}{\partial \delta_N} & |V_2|\frac{\partial P_N}{\partial |V_2|} & \cdots & |V_N|\frac{\partial P_N}{\partial |V_N|} & 0 \\ \frac{\partial Q_2}{\partial \delta_2} & \cdots & \frac{\partial Q_2}{\partial \delta_m} & \cdots & \frac{\partial Q_2}{\partial \delta_N} & |V_2|\frac{\partial Q_2}{\partial |V_2|} & \cdots & |V_N|\frac{\partial Q_2}{\partial |V_N|} & \vdots \\ \vdots & \vdots & \vdots & \vdots & \vdots & \vdots & \vdots & \vdots & \vdots \\ \frac{\partial Q_N}{\partial \delta_2} & \cdots & \frac{\partial Q_N}{\partial \delta_m} & \cdots & \frac{\partial Q_N}{\partial \delta_N} & |V_2|\frac{\partial Q_N}{\partial |V_2|} & \cdots & |V_N|\frac{\partial Q_N}{\partial |V_N|} & 0 \\ \frac{\partial Q_m}{\partial \delta_2} & \cdots & \frac{\partial Q_N}{\partial \delta_m} & \cdots & \frac{\partial Q_m}{\partial \delta_N} & |V_2|\frac{\partial Q_m}{\partial |V_2|} & \cdots & |V_N|\frac{\partial Q_m}{\partial |V_N|} & \frac{\partial Q_m}{\partial \alpha} \end{bmatrix} \begin{bmatrix} \Delta \delta_2 \\ \vdots \\ \Delta \delta_m \\ \vdots \\ \Delta \delta_N \\ \frac{\Delta |V_2|}{|V_2|} \\ \vdots \\ \frac{\Delta |V_N|}{|V_N|} \\ \Delta \alpha \end{bmatrix} \quad (1)$$

At the end of i^{th} iteration, the variable firing angle α is updated like other state variables as,

$$\alpha^{i+1} = \alpha^{i} + \Delta\alpha^{i} \tag{2}$$

2.2 Static Synchronous Compensator

STATCOM is a voltage source converter (VSC) based FACTS-device which consists of a coupling transformer, an inverter and a DC capacitor as shown in Figure 2. STATCOM controls transmission voltage by reactive power shunt compensation and therefore the active power flow to the DC part of the STATCOM can be neglected. Harmonics generated by the STATCOM are also neglected here. Then the STATCOM can be equivalently represented by a controllable fundamental frequency positive sequence voltage source [20]. In principle, the STATCOM output voltage can be regulated such that the reactive power injected or absorbed by the STATCOM can be changed.

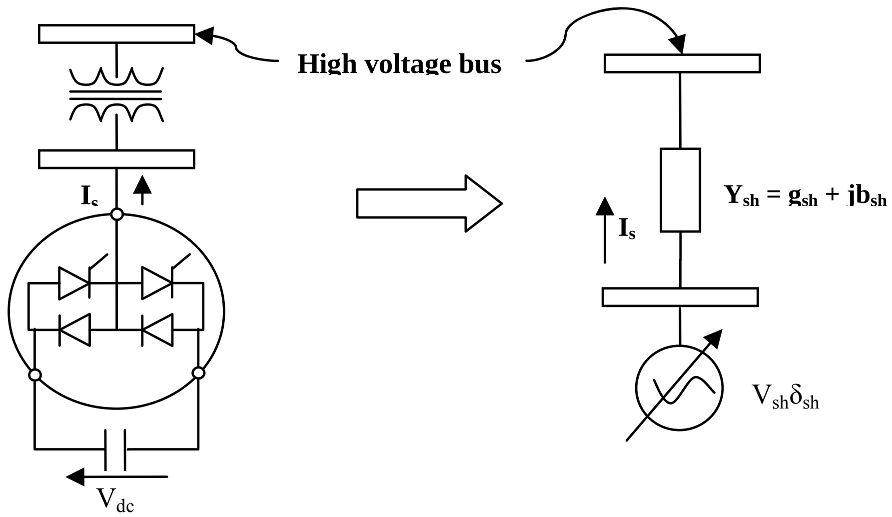

Fig.2. STATCOM connected to transmission network via coupling transformer

In order to develop a mathematical model of STATCOM for NR power flow, a separate bus with controllable voltage magnitude and angle ($V_{sh}\angle\delta_{sh}$) i.e. a controllable voltage source is assumed to be connected to bus of the power network via an impedance due to the coupling transformer $Z_{sh}=R_{sh} + jX_{sh}$, where V_{sh} is proportional to V_{dc} (capacitor voltage) of the STATCOM. The bus of the power network to which the STATCOM is connected is now modelled as a specially controlled PV bus where the active and reactive power injections and the voltage magnitude are specified, while the voltage phase angle of ac system bus, control angle and ac voltage of STATCOM is treated as the state variables in its place.

The limits on the ac current I_s, phase angle $\angle\delta_{sh}$ and ac voltage V_{sh}, can be directly introduced in this mathematical model of STATCOM. The current limit being the main limiting factor in VSC-based devices, this has been enforced when either the maximum limit $I_{s\,max}$ or minimum limit $I_{s\,min}$ is reached, depending on whether the controller is operating in the inductive or capacitive domain. Thus on violation of these limits the bus of the power network to which the STATCOM is connected is modelled as a PQ bus, where the ac current I_s, the active and reactive power injections are specified, while the voltage magnitude, angle of ac system bus, control angle and the ac voltage of STATCOM are treated as the state variables in its place.

Let the STATCOM be connected to the i^{th} bus of the power system, then the power flow constraints of the STATCOM are [17]:

$$P_i = \left|V_i^2\right| g_{sh} - |V_i||V_{sh}| g_{sh} \cos(\delta_i - \delta_{sh}) - |V_i||V_{sh}| b_{sh} \sin(\delta_i - \delta_{sh})$$

$$Q_i = -\left|V_i^2\right| b_{sh} - |V_i||V_{sh}| g_{sh} \sin(\delta_i - \delta_{sh}) + |V_i||V_{sh}| b_{sh} \cos(\delta_i - \delta_{sh})$$

where $(g_{sh} + jb_{sh}) = 1/Z_{sh}$

The operating constraint of the STATCOM is the active power exchange via the DC-link as described by:

$$P_{sh} = \left|V_{sh}^2\right| g_{sh} - |V_i||V_{sh}| g_{sh} \cos(\delta_{sh} - \delta_i) - |V_i||V_{sh}| b_{sh} \sin(\delta_{sh} - \delta_i) \tag{3}$$

The partial derivatives required for power flow equations when ac current I_s is within its limits, are given by:

$$\frac{\partial P_i}{\partial |V_{sh}|}|V_{sh}| = -|V_i||V_{sh}| g_{sh} \cos(\delta_i - \delta_{sh}) - |V_i||V_{sh}| b_{sh} \sin(\delta_i - \delta_{sh})$$

$$\frac{\partial Q_i}{\partial |V_{sh}|}|V_{sh}| = -|V_i||V_{sh}| g_{sh} \sin(\delta_i - \delta_{sh}) + |V_i||V_{sh}| b_{sh} \cos(\delta_i - \delta_{sh})$$

$$\frac{\partial P_i}{\partial \delta_{sh}} = -|V_i||V_{sh}| g_{sh} \sin(\delta_i - \delta_{sh}) + |V_i||V_{sh}| b_{sh} \cos(\delta_i - \delta_{sh})$$

$$\frac{\partial Q_i}{\partial \delta_{sh}} = |V_i||V_{sh}| g_{sh} \cos(\delta_i - \delta_{sh}) + |V_i||V_{sh}| b_{sh} \sin(\delta_i - \delta_{sh})$$

$$\frac{\partial P_{sh}}{\partial \delta_i} = -|V_i||V_{sh}| g_{sh} \sin(\delta_{sh} - \delta_i) + |V_i||V_{sh}| b_{sh} \cos(\delta_{sh} - \delta_i)$$

$$\frac{\partial P_{sh}}{\partial |V_{sh}|}|V_{sh}| = 2|V_{sh}|^2 g_{sh} - |V_i||V_{sh}| g_{sh} \cos(\delta_{sh} - \delta_i) - |V_i||V_{sh}| b_{sh} \sin(\delta_{sh} - \delta_i)$$

$$\frac{\partial P_{sh}}{\partial \delta_{sh}} = |V_i||V_{sh}| g_{sh} \sin(\delta_{sh} - \delta_i) - |V_i||V_{sh}| b_{sh} \cos(\delta_{sh} - \delta_i)$$

The linearized power flow equations in matrix form are given by:

$$
\begin{bmatrix} \Delta P_2 \\ \vdots \\ \Delta P_i \\ \vdots \\ \Delta P_N \\ \Delta Q_2 \\ \vdots \\ \Delta Q_N \\ \Delta Q_i \\ \Delta P_{sh} \end{bmatrix} =
\begin{bmatrix}
\frac{\partial P_2}{\partial \delta_2} & \cdots & \frac{\partial P_2}{\partial \delta_i} & \cdots & \frac{\partial P_2}{\partial \delta_N} & |V_2|\frac{\partial P_2}{\partial |V_2|} & \cdots & |V_N|\frac{\partial P_2}{\partial |V_N|} & 0 & 0 \\
\vdots & & \vdots & & \vdots & \vdots & & \vdots & \vdots & \vdots \\
\frac{\partial P_i}{\partial \delta_2} & \cdots & \frac{\partial P_i}{\partial \delta_i} & \cdots & \frac{\partial P_i}{\partial \delta_N} & |V_2|\frac{\partial P_i}{\partial |V_2|} & \cdots & |V_N|\frac{\partial P_i}{\partial |V_N|} & |V_{sh}|\frac{\partial P_i}{\partial |V_{sh}|} & \frac{\partial P_i}{\partial \delta_{sh}} \\
\vdots & & \vdots & & \vdots & \vdots & & \vdots & \vdots & \vdots \\
\frac{\partial P_N}{\partial \delta_2} & \cdots & \frac{\partial P_N}{\partial \delta_i} & \cdots & \frac{\partial P_N}{\partial \delta_N} & |V_2|\frac{\partial P_N}{\partial |V_2|} & \cdots & |V_N|\frac{\partial P_N}{\partial |V_N|} & 0 & 0 \\
\frac{\partial Q_2}{\partial \delta_2} & \cdots & \frac{\partial Q_2}{\partial \delta_i} & \cdots & \frac{\partial Q_2}{\partial \delta_N} & |V_2|\frac{\partial Q_2}{\partial |V_2|} & \cdots & |V_N|\frac{\partial Q_2}{\partial |V_N|} & 0 & 0 \\
\vdots & & \vdots & & \vdots & \vdots & & \vdots & \vdots & \vdots \\
\frac{\partial Q_N}{\partial \delta_2} & \cdots & \frac{\partial Q_N}{\partial \delta_i} & \cdots & \frac{\partial Q_N}{\partial \delta_N} & \frac{\partial Q_N}{\partial \delta_N} & \cdots & |V_N|\frac{\partial Q_N}{\partial |V_N|} & 0 & 0 \\
\frac{\partial Q_i}{\partial \delta_2} & \cdots & \frac{\partial Q_i}{\partial \delta_i} & \cdots & \frac{\partial Q_i}{\partial \delta_N} & \frac{\partial Q_i}{\partial \delta_N} & \cdots & |V_N|\frac{\partial Q_i}{\partial |V_N|} & |V_{sh}|\frac{\partial Q_i}{\partial |V_{sh}|} & \frac{\partial Q_i}{\partial \delta_{sh}} \\
0 & \cdots & \frac{\partial P_{sh}}{\partial \delta_i} & \cdots & 0 & 0 & \cdots & 0 & |V_{sh}|\frac{\partial P_{sh}}{\partial |V_{sh}|} & \frac{\partial P_{sh}}{\partial \delta_{sh}}
\end{bmatrix}
\begin{bmatrix} \Delta \delta_2 \\ \vdots \\ \Delta \delta_i \\ \vdots \\ \Delta \delta_N \\ \frac{\Delta |V_2|}{|V_2|} \\ \vdots \\ \frac{\Delta |V_N|}{|V_N|} \\ \frac{\Delta |V_{sh}|}{|V_{sh}|} \\ \Delta \delta_{sh} \end{bmatrix} \tag{4}
$$

At the end of the i[th] iteration, the variable voltage magnitude and phase angle is updated like other state variables as,

$$ |V_{sh}|^{i+1} = |V_{sh}|^{i} \left[1 + \left(\frac{\Delta |V_{sh}|}{|V_{sh}|} \right)^{i} \right] \tag{5} $$

and $$ \delta_{sh}^{i+1} = \delta_{sh}^{i} + \Delta \delta_{sh}^{i} \tag{6} $$

However if the current, $I_s = \frac{|V_i|\angle\delta_i - |V_{sh}|\angle\delta_{sh}}{Z_{sh}}$ is not within the specified limits, then I_s is fixed at the respective limits. In this control mode, the control constraint may be represented by $I_s - I_{s\_spec} = 0$. However it is found that there are two solutions corresponding to this control constraint. Due to the problem incurred, the power flow solution with such a constraint may arbitrarily converge to one of the two solutions. In order to avoid the above non-unique solution problem, an alternative formulation of the current magnitude control is used. Since P_{sh}=0 is a constraint in the modelling thus I_s leads V_{sh} by 90^0 in capacitive mode and lags it by 90^0 in inductive mode. So, we can write the following constraints [17, 20]:

For Capacitive Compensation,

$$ \mathrm{Re}\left[I_{s\_spec} \angle\left(\delta_{sh} + 90^0\right) \right] = \mathrm{Re}\left[\frac{|V_i|\angle\delta_i - |V_{sh}|\angle\delta_{sh}}{Z_{sh}} \right] \text{ or } \mathrm{Im}\left[I_{s\_spec} \angle\left(\delta_{sh} + 90^0\right) \right] = \mathrm{Im}\left[\frac{|V_i|\angle\delta_i - |V_{sh}|\angle\delta_{sh}}{Z_{sh}} \right] $$

For Inductive Compensation,

$$ \mathrm{Re}\left[I_{s\_spec} \angle\left(\delta_{sh} - 90^0\right) \right] = \mathrm{Re}\left[\frac{|V_i|\angle\delta_i - |V_{sh}|\angle\delta_{sh}}{Z_{sh}} \right] \text{ or } \mathrm{Im}\left[I_{s\_spec} \angle\left(\delta_{sh} - 90^0\right) \right] = \mathrm{Im}\left[\frac{|V_i|\angle\delta_i - |V_{sh}|\angle\delta_{sh}}{Z_{sh}} \right] $$

As the STATCOM operation violates its current limit the operational equation changes to difference of real parts of specified and calculated current injected by it,

$$I_{net} = \left(|V_i| cos\,\delta_i - |V_{sh}| cos\,\delta_{sh}\right) g_{sh} - \left(|V_i| sin\,\delta_i - |V_{sh}| sin\,\delta_{sh}\right) b_{sh} - I_{s\_spec}\, cos\left(\delta_{sh} + 90^0\right) \quad (7)$$

The partial derivatives of the power flow equations required are:

$$\frac{\partial P_{sh}}{\partial |V_i|}|V_i| = -|V_i||V_{sh}| g_{sh}\, cos(\delta_{sh} - \delta_i) - |V_i||V_{sh}| b_{sh}\, sin(\delta_{sh} - \delta_i)$$

$$\frac{\partial I_{net}}{\partial |V_i|}|V_i| = |V_i| g_{sh}\, cos\,\delta_i - |V_i| b_{sh}\, sin\,\delta_i$$

$$\frac{\partial I_{net}}{\partial |V_{sh}|}|V_{sh}| = -|V_{sh}| g_{sh}\, cos\,\delta_{sh} + |V_{sh}| b_{sh}\, sin\,\delta_{sh}$$

$$\frac{\partial I_{net}}{\partial \delta_i} = -|V_i| g_{sh}\, sin\,\delta_i - |V_i| b_{sh}\, cos\,\delta_i$$

$$\frac{\partial I_{net}}{\partial \delta_{sh}} = |V_{sh}| g_{sh}\, sin\,\delta_{sh} + |V_{sh}| b_{sh}\, cos\,\delta_{sh} + I_{s\_spec}\, sin\left(\delta_{sh} + 90^0\right)$$

The linearized power flow equations are:

$$\begin{bmatrix} \Delta P_2 \\ \vdots \\ \Delta P_i \\ \vdots \\ \Delta P_N \\ \vdots \\ \Delta Q_i \\ \vdots \\ \Delta Q_N \\ \Delta I_{net} \\ \Delta P_{sh} \end{bmatrix} = \begin{bmatrix} \frac{\partial P_2}{\partial \delta_2} & \cdots & \frac{\partial P_2}{\partial \delta_i} & \cdots & \frac{\partial P_2}{\partial \delta_N} & \cdots & |V_i|\frac{\partial P_2}{\partial |V_i|} & \cdots & |V_N|\frac{\partial P_2}{\partial |V_N|} & 0 & 0 \\ \vdots & & \vdots & & \vdots & & \vdots & & \vdots & \vdots & \vdots \\ \frac{\partial P_i}{\partial \delta_2} & \cdots & \frac{\partial P_i}{\partial \delta_i} & \cdots & \frac{\partial P_i}{\partial \delta_N} & \cdots & |V_i|\frac{\partial P_i}{\partial |V_i|} & \cdots & |V_N|\frac{\partial P_i}{\partial |V_N|} & |V_{sh}|\frac{\partial P_i}{\partial |V_{sh}|} & \frac{\partial P_i}{\partial \delta_{sh}} \\ \vdots & & \vdots & & \vdots & & \vdots & & \vdots & 0 & 0 \\ \frac{\partial P_N}{\partial \delta_2} & \cdots & \frac{\partial P_N}{\partial \delta_i} & \cdots & \frac{\partial P_N}{\partial \delta_N} & \cdots & |V_i|\frac{\partial P_N}{\partial |V_i|} & \cdots & |V_N|\frac{\partial P_N}{\partial |V_N|} & 0 & 0 \\ \vdots & & \vdots & & \vdots & & \vdots & & \vdots & \vdots & \vdots \\ \frac{\partial Q_i}{\partial \delta_2} & \cdots & \frac{\partial Q_i}{\partial \delta_i} & \cdots & \frac{\partial Q_i}{\partial \delta_N} & \cdots & |V_i|\frac{\partial Q_i}{\partial |V_i|} & \cdots & |V_N|\frac{\partial Q_i}{\partial |V_N|} & |V_{sh}|\frac{\partial Q_i}{\partial |V_{sh}|} & \frac{\partial Q_i}{\partial \delta_{sh}} \\ \vdots & & \vdots & & \vdots & & \vdots & & \vdots & \vdots & \vdots \\ \frac{\partial Q_N}{\partial \delta_2} & \cdots & \frac{\partial Q_N}{\partial \delta_i} & \cdots & \frac{\partial Q_N}{\partial \delta_N} & \cdots & |V_i|\frac{\partial Q_N}{\partial |V_i|} & \cdots & |V_N|\frac{\partial Q_N}{\partial |V_N|} & 0 & 0 \\ 0 & \cdots & \frac{\partial I_{net}}{\partial \delta_i} & \cdots & 0 & \cdots & |V_i|\frac{\partial I_{net}}{\partial |V_i|} & \cdots & 0 & |V_{sh}|\frac{\partial I_{net}}{\partial |V_{sh}|} & \frac{\partial I_{net}}{\partial \delta_{sh}} \\ 0 & \cdots & \frac{\partial P_{sh}}{\partial \delta_i} & \cdots & 0 & \cdots & |V_i|\frac{\partial P_{sh}}{\partial |V_i|} & \cdots & 0 & |V_{sh}|\frac{\partial P_{sh}}{\partial |V_{sh}|} & \frac{\partial P_{sh}}{\partial \delta_{sh}} \end{bmatrix} \begin{bmatrix} \Delta \delta_2 \\ \vdots \\ \Delta \delta_i \\ \vdots \\ \Delta \delta_N \\ \vdots \\ \frac{\Delta |V_i|}{|V_i|} \\ \vdots \\ \frac{\Delta |V_N|}{|V_N|} \\ \frac{\Delta |V_{sh}|}{|V_{sh}|} \\ \Delta \delta_{sh} \end{bmatrix} \quad (8)$$

The state variables are updated as stated earlier.

3. Equivalent two-bus model and formulation of global voltage stability index

Two-bus equivalent model for any multi-bus power system is obtained using the total active and reactive load and loss available from load flow analysis for a particular operating condition where none of the two buses are actually present in the system as in [12-16] as shown in Fig. 3.

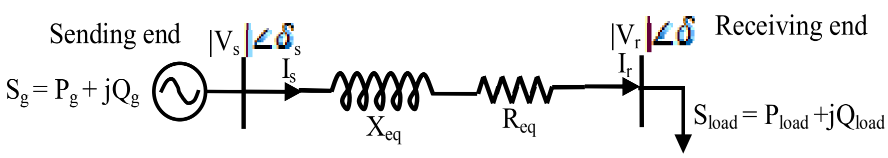

Fig.3. Two-bus series equivalent network

The power balance equation for the two-bus equivalent network can be written as

$S_g = S_{loss} + S_{load}$ i.e., $P_g + jQ_g = \overrightarrow{V_s}\overrightarrow{I_s^*} = P_{loss} + jQ_{loss} + P_{load} + jQ_{load}$

$$|\overline{I_s}|^2 = \frac{P_g^2 + Q_g^2}{|\overline{V_s}|^2}$$

So, $$r_{eq} = \frac{P_{loss}}{|\overline{I_s}|^2} = \frac{P_{loss}}{\left(P_g^2 + Q_g^2\right)}|\overline{V_s}|^2 \quad \text{and} \quad x_{eq} = \frac{Q_{loss}}{|\overline{I_s}|^2} = \frac{Q_{loss}}{\left(P_g^2 + Q_g^2\right)}|\overline{V_s}|^2 \tag{9}$$

$$\overline{V_r} = \overline{V_s} - \left(r_{eq} + jx_{eq}\right)\frac{\left(P_g - jQ_g\right)}{\overline{V_s^*}}$$

Where V_s, V_r and I_s, I_r are the sending and receiving end voltages and currents; S_g, S_{load} are the total complex source and load powers respectively. S_{loss} is the total complex loss in the power system.

Assuming $\overline{V_s}$ to be at nominal value of $1\angle 0^\circ$ p.u., we get

$$r_{eq} = \frac{P_{loss}}{\left(P_g^2 + Q_g^2\right)} \quad ; \quad x_{eq} = \frac{Q_{loss}}{\left(P_g^2 + Q_g^2\right)}$$

Thus the two-bus system described above becomes the equivalent model of a multi-bus network at any particular network and load configuration where the total interconnected system has been replaced by a single line two bus system with same generation, load and loss. The parameters of the equivalent model will obviously vary with change in load pattern or with change in any system configuration.

Once the global two-bus power network equivalent to multi-bus power system is obtained, then the global voltage stability index (GVSI) could be formulated in a straight forward manner from parameters of the global network as described below [16]:

From equation (9),

$$r_{eq} = \frac{P_{loss}}{|\overline{I_s}|^2} = \frac{P_{loss}}{\left(P_g^2 + Q_g^2\right)}|\overline{V_s}|^2 \ , \ x_{eq} = \frac{Q_{loss}}{|\overline{I_s}|^2} = \frac{Q_{loss}}{\left(P_g^2 + Q_g^2\right)}|\overline{V_s}|^2$$

$$P_g = r_{eq}\frac{\left(P_g^2 + Q_g^2\right)}{|\overline{V_s}|^2} + P_{load} \quad \text{and} \quad Q_g = x_{eq}\frac{\left(P_g^2 + Q_g^2\right)}{|\overline{V_s}|^2} + Q_{load}$$

or, $$Q_g = \frac{\left(P_g - P_{load}\right)x_{eq} + r_{eq}Q_{load}}{r_{eq}}$$

Replacing Q_g in the equation of P_g ,

$$P_g = \frac{r_{eq}\left[P_g^2 + \left\{\frac{x_{eq}\left(P_g - P_{load}\right) + r_{eq}Q_{load}}{r_{eq}}\right\}^2\right]}{\left|\overline{V}_s\right|^2} + P_{load}$$

which for $\left|\overline{V}_s\right| = 1$ becomes,

$$\therefore \; P_g^2\left(r_{eq}^2 + x_{eq}^2\right) - \left(2x_{eq}^2 P_{load} - 2r_{eq}x_{eq}Q_{load} + r_{eq}\right)P_g + \left(x_{eq}^2 P_{load}^2 + r_{eq}^2 Q_{load}^2 - 2r_{eq}x_{eq}P_{load}Q_{load} + r_{eq}P_{load}\right) = 0 \qquad (10)$$

$$i.e. \; P_{g_{1,2}} = \frac{\left(2x_{eq}^2 P_{load} - 2r_{eq}x_{eq}Q_{load} + r_{eq}\right)}{2\left(r_{eq}^2 + x_{eq}^2\right)} \pm \frac{\sqrt{\left(2x_{eq}^2 P_{load} - 2r_{eq}x_{eq}Q_{load} + r_{eq}\right)^2 - 4\left(r_{eq}^2 + x_{eq}^2\right)\left(x_{eq}^2 P_{load}^2 + r_{eq}^2 Q_{load}^2 - 2r_{eq}x_{eq}P_{load}Q_{load} + r_{eq}P_{load}\right)}}{2\left(r_{eq}^2 + x_{eq}^2\right)} \qquad (11)$$

Now, P_g must have a real value, hence the discriminant of equation (11) must be greater than or equal to zero. This yields the following relation:

$$\left(2x_{eq}^2 P_{load} - 2r_{eq}x_{eq}Q_{load} + r_{eq}\right)^2 - 4\left(r_{eq}^2 + x_{eq}^2\right)\left(x_{eq}^2 P_{load}^2 + r_{eq}^2 Q_{load}^2 - 2r_{eq}x_{eq}P_{load}Q_{load} + r_{eq}P_{load}\right) \geq 0$$

$$\therefore \quad 4\left\{\left(x_{eq}P_{load} - r_{eq}Q_{load}\right)^2 + x_{eq}Q_{load} + r_{eq}P_{load}\right\} \leq 1 \qquad (12)$$

Above expression is termed as Global Voltage Stability Index (GVSI) which gradually increases with increasing load in the actual power system and reach the value ‘1’ at critical point of voltage stability (when load flow matrix Jacobian becomes singular). Therefore the value of GVSI is used to indicate how for the present operating condition is from the global system voltage collapse i.e., the global voltage stability margin and so to assess the overall voltage stability status of a multi-bus power system at a particular operating point.

4. Computational Algorithm

The necessary algorithm for the system simulation is given below:

1. Solve Newton-Raphson power flow for base case load and determine the weakest bus of the given multi-bus system.
2. Make necessary changes in the admittance matrix and Jacobian for incorporating contingency, SVC or STATCOM.
3. Solve power flow problem to obtain the system states. Go to step 6 if load flow iterative process does not converge.

4. Calculate the total generation, load and transmission line loss of the system. Calculate equivalent resistance (r_{eq}) and reactance (x_{eq}) for the two-bus equivalent model and hence global voltage stability index.
5. Increase the load of weakest bus in small steps at a constant power factor and go to step-3.
6. Stop.

5. Simulation results

A computer software programme has been developed in the MATLAB environment to perform the Newton-Raphson load flow analysis including the above discussed models of SVC and STATCOM on standard IEEE 57-bus system. The system has a base load of 1295.14 MVA with 4 generators and 3 synchronous compensators and the weakest bus being bus no. 31 according to reactive power sensitivity analysis [21].

First, the power flow problem of the system is successively solved for uniformly increasing load conditions (at an increment of 20% of base value keeping the load power factor constant) at the weakest bus until the power flow algorithm fails to converge, indicating voltage instability as no possible system voltages are available. The Power flow problems are then similarly solved for application of a SVC or STATCOM (only one at a time) at the weakest bus. For each case of system simulation and for each load set, the two bus series-equivalent model parameters have been calculated and have been used to calculate the Global Voltage Stability Index (GVSI). It should be clear that the load increase is possible with any one or more bus in the system. Weakest bus of system is considered here only to describe the methodology in better way as weakest bus in terms of reactive power sensitivity is most vulnerable to voltage collapse. In practical case the FACTS controllers may be connected to any bus of the power system as per requirement.

The SVC parameters adopted are: 1) Transformer reactance X_t=0.334 p.u., 2) Transformer resistance R_t =0, 3) Inductor reactance for the TCR, X_L=0.8741 p.u. and 4) The capacitive reactance, X_C=3.2484 p.u. The maximum capacitive susceptance obtained is B_{SVC_max} = 0.3431 p.u. i.e. 34.31 MVar is the maximum reactive power that the SVC can inject at 1.00 p.u. terminal voltage. Resonance for the values adopted for the SVC model occurs at about 128^0. Thus an initial value of 140^0 has been adopted for the firing angle α.

The STATCOM rating is chosen such that the maximum capacitive current is equal to 0.3431 p.u. such that maximum reactive power injected is 34.31 MVar at 1.00 p.u. terminal voltage. The transformer reactance connecting the STATCOM to the system bus is chosen as 0.1 p.u.

Fig. 4 exhibits the profile of Global Voltage Stability Index for 57-bus system indicating that the system gradually moves towards voltage instability with increase in load as well as it is clear that with the application of SVC or STATCOM at weakest bus of the system, the GVSI has been improved with better load catering capability. Contingency at lines 30-31 & 32-31 have been alternatively simulated with and without SVC or STATCOM connected to the weakest bus to indicate the system response. In all type of system operation STATCOM helps in better system performance as compared to SVC.

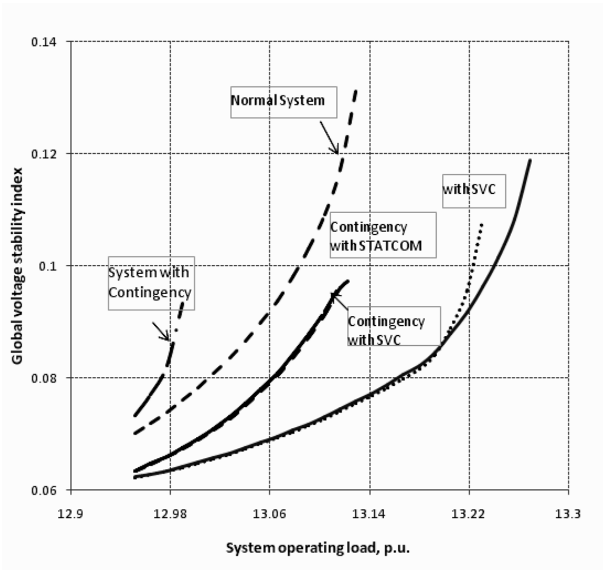

Fig.4. Variation in GVSI for different operating conditions

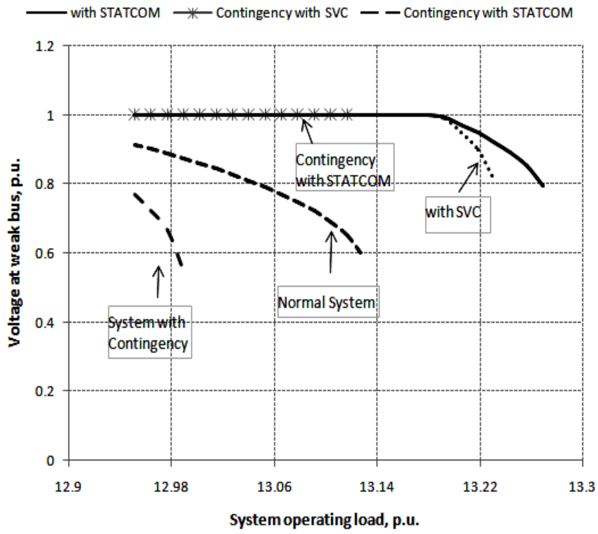

Fig.5. Variation in weak bus voltage for different operating conditions

This is clear that the value of GVSI will not reach 1 at the maximum loading point as it has been calculated from equivalent two bus system of the original network and for which series admittance varies with variation in system operating condition. Still a set of pre-calculated values of GVSI corresponds to the collapse points for different operating condition may be useful for real time operation where only the total line loss, total generation and total load of entire system will be sufficient for calculating the present indicator value from measured system data which on comparison with the already pre-calculated GVSI data may reveal whether the system is at the verge of voltage collapse or not almost instantaneously. Thus this approach may be beneficial due to its simplicity associated with high speed of decision making.

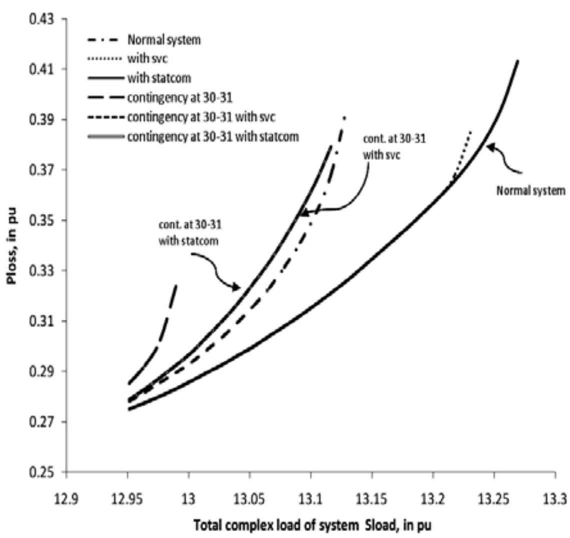

Fig.6. Variation of active power loss for different operating conditions

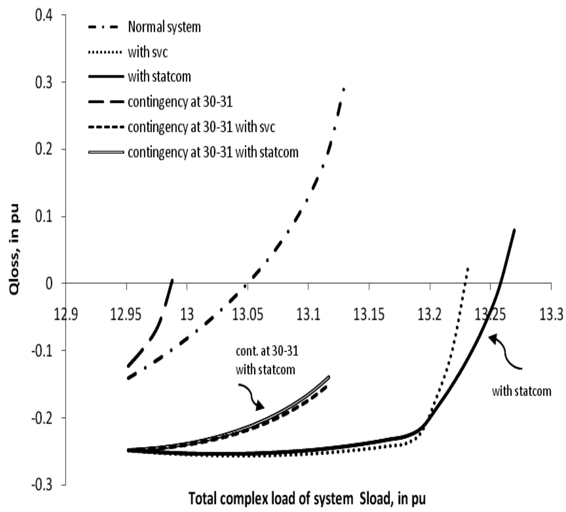

Fig.7. Variation of reactive power loss for different operating conditions

The bus voltage magnitude in Fig. 5 reveals that the voltage corresponding to the weakest bus gradually decreasing and thereby it approaches voltage instability for increase in system loading. A flatter voltage profile is possible where SVC/STATCOM is connected at the weakest bus of the system with better load handling capacity. Bus voltage starts drooping when SVC reaches its firing angle limit. For STATCOM application bus voltage become incontrollable when STATCOM reaches it current limit. STATCOM is capable to hold bus voltage constant for higher range of system load as compared to SVC.

Figs. 6 and 7 clearly demonstrate that active and reactive power losses are reduced in a better way due installation of STATCOM as compared to SVC under every operating condition for both of the test system.

6. Conclusion

A global voltage security index derived from the two bus equivalent of any multi-bus power system provides an overall view regarding voltage stability status of the system and thus helps the system operator to opt for suitable corrective measures on the verge of system voltage stability. The GVSI has high potential for on line application even with line contingencies and in the presence of FACTS devices. Among SVC and STATCOM, the second one provides better control over voltage stability and secures the voltage stable states in better way in all stages of system operation.

References

[1] V. Ajjarapu & B. Lee, Bibliography on voltage stability, *IEEE Transactions on Power Systems*, *13*(1), 1990, 115-125.

[2] T. V. Cutsem & C. Vournas, Voltage stability of electrical power systems, *Kluwer Academic Publishers*, USA, 2003.

[3] M. De & S. K. Goswami, Reactive power cost allocation by power tracing based method, *Energy Conservation and Management*, 64, 2012, 43-51.

[4] P. W. Sauer & M. A. Pai, Power system steady state stability and the load flow Jacobian, *IEEE Transactions on Power Systems*, *5*(4), 1990, 1374-1383.

[5] B. Gao, G. K. Morison & P. Kundur, Voltage stability evaluation using modal analysis, *IEEE Transactions on Power Systems*, *7*, 1992, 1529-1542.

[6] P. B. Chitare, V. S. K. Murthy Balijepalli & S. A. Khaparde, Online assessment of voltage stability in power systems with PMUs, *International Journal of Emerging Electric Power Systems*, *14*(2), 2013, 115-122.

[7] E. Vaahedi, J. Tamby, Y. Mansour, W. Li & D. Sun, Large scale voltage stability constrained optimal VAR planning and voltage stability applications using existing OPF/optimal VAR planning tools, *IEEE Transactions on Power Systems*, *14*(1), 1999, 65-74.

[8] P. Nagendra, T. Datta, S. Halder & S. Paul, Power system voltage stability assessment using network equivalents- a review, *Journal of Applied Sciences*, *10*(18), 2010, 2147-2153.

[9] A. M. Chebbo, M. R. Irving & M. J. H. Sterling, Voltage collapse proximity indicator: behaviour and implications, *IEE Proc.-C Generation, Transmission and Distribution*, *139*, 1992, 241-252.

[10] M. H. Haque, A fast method for determining the voltage stability limit of a power system, *Electrical Power Systems Research*, *32*, 1995, 35-43.

[11] A. Wiszniewski, New criteria of voltage stability margin for the purpose of load shedding, *IEEE Power Transactions on Power Delivery*, *22*, 2007, 1367-1371.

[12] G. B. Jasmon & L. H. C. C. Lee, Distribution network reduction for voltage stability analysis and load flow calculation, *International Journal of Electric Power and Energy System*, *13*(1), 1991, 9-13.

[13] P. Nagendra, S. Halder nee Dey, S. Paul & T. Datta, OPF based global voltage stability assessment of a practical power system incorporating TCSC controller, *Journal of Electrical Systems*, *7*(1), 2011, 101-110.

[14] P. Nagendra, S. Halder nee Dey, S. Paul & T. Datta, An innovative technique to evaluate network equivalent for voltage stability assessment in a widespread sub-grid system, *International Journal of Electric Power and Energy System*, *33*(3), 2011, 737-744.

[15] K. Chakraborty, A. De & A. Chakrabarti, Assessment of voltage security in a multi-bus power system using artificial neural network and voltage stability indicators, *Journal of Electrical Systems*, 6(4), 2010, 517-529.
[16] P. Nagendra, OPF based voltage stability analysis of multi-bus power system with FACTS controllers, Ph.D. Thesis, Jadavpur University, Kolkata, India, 2011.
[17] Z. Xiao-Ping, C. Rehtanz & B. Pal, Flexible Ac transmission systems: Modelling and control, Springer, 2006.
[18] H. Ambriz-Perez, E. Acha & C. R. Fuerte-Esquivel, Advanced SVC models for Newton-Raphson load flow and Newton optimal power flow studies, *IEEE Transactions on Power Systems*, *15*, 2000, 129-136.
[19] P. Nagendra, S. Halder nee Dey, S. Paul & T. Datta, A novel approach for global voltage stability assessment of a power system incorporating static var compensator, *European Transactions on Electrical Power*, 22, 2012, 1016-1026.
[20] Y. Zhang, B. Wu & J. Zhou, Power injection model of STATCOM with control and operating limit for power flow and voltage stability analysis, *Electrical Power Systems Research*, *76*, 2006, 1003-1010.
[21] T. V. Cutsem, An approach to corrective control of voltage instability using simulation and sensitivity, *IEEE Transactions on Power Systems*, *10*, 1995, 616-622.

Appendix

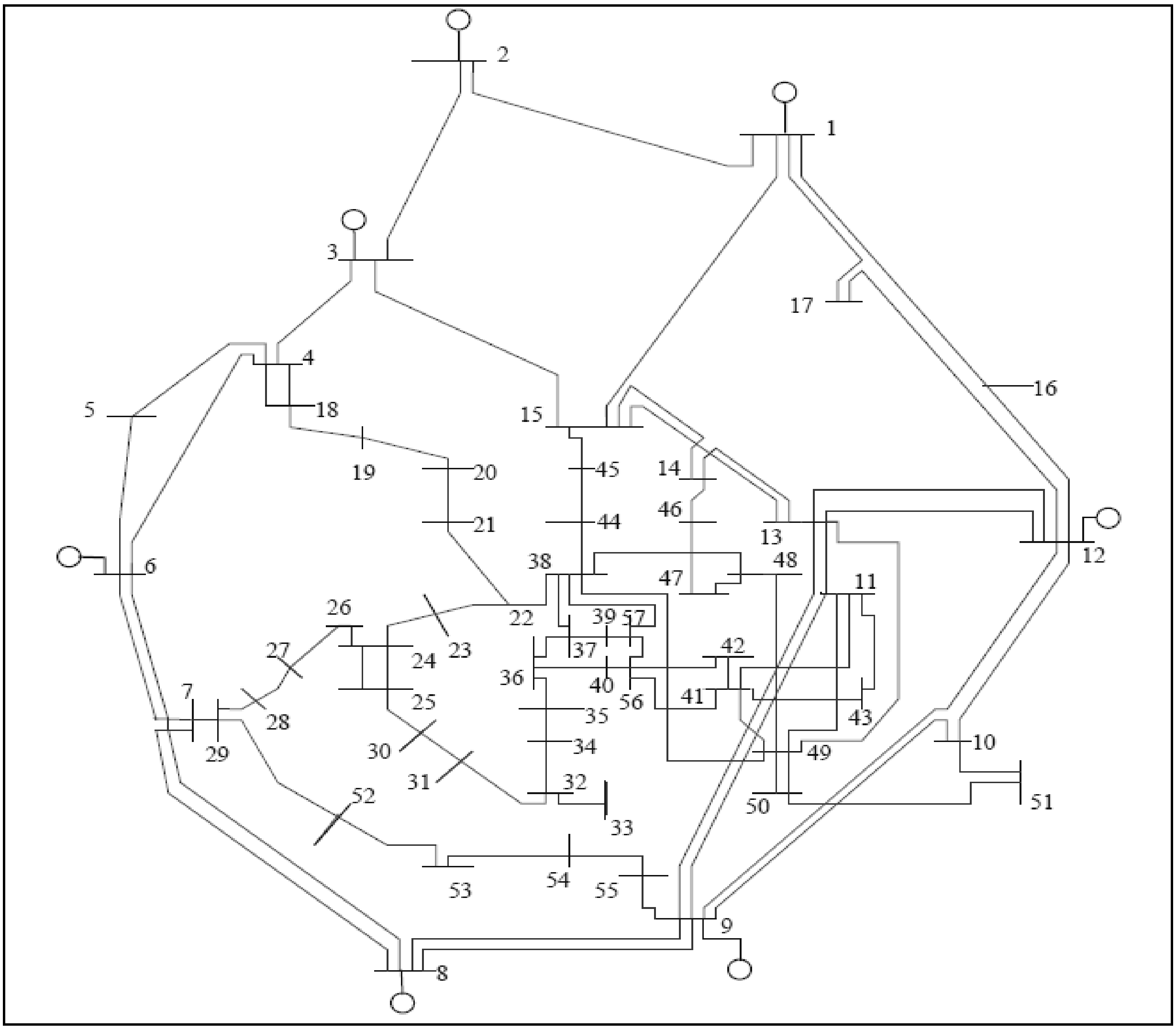

Single line diagram of IEEE 57-bus test system